INTERNATIONAL JOURNAL OF ACADEMIC RESEARCH IN BUSINESS & SOCIAL SCIENCES

Vol 15, Issue 2, (2025) E-ISSN: 2222-6990

Investigating the Flexibility of ZnO Nanorod Growth Parameters for Humidity Sensor Design

Haziezol Helmi Mohd Yusof[1], Abd Majid Darsono[1], Hazli Rafis Abdul Rahim[1], Kaharudin Dimyati[2], Sulaiman Wadi Harun[2]

[1]Fakulti Teknologi dan Kejuruteraan Elektronik dan Komputer, Universiti Teknikal Malaysia Melaka, Jalan Hang Tuah Jaya, 76100 Durian Tunggal, Melaka, Malaysia, [2]Jabatan Kejuruteraan Elektrik, Fakulti Kejuruteraan, Universiti Malaya, 50603 Kuala Lumpur, Malaysia

Corresponding Author Email: haziezol@utem.edu.my

To Link this Article: http://dx.doi.org/10.6007/IJARBSS/v15-i2/24753 DOI:10.6007/IJARBSS/v15-i2/24753

Published Date: 10 February 2025

Abstract

A study on the effect of ZnO nanorod growth conditions on humidity sensing is presented. Glass substrates were coated with triangular ZnO nanorods using a hydrothermal method, with growth durations of 5, 10, and 15 hours, and coating lengths in triangular shape varying from 1 mm to 13 mm. A commercial LED and photodiode were utilized in the measurement setup, functioning as the light source and photodetector, respectively, and interfaced with an Arduino for data processing. Humidity experiments were conducted in a controlled chamber using different combinations of these growth parameters. The results indicated that a combination of 10 hours growth time and 7 mm coating length produced a sensing response comparable to that of a 15-hour growth time and 4 mm coating length at 80% relative humidity. This demonstrates that optimal sensor performance can be achieved through various fabrication settings, suggesting that flexibility in process parameters allows for more efficient and cost-effective sensor design without sacrificing the sensor performance. By offering multiple viable fabrication paths, the process becomes more scalable and versatile, allowing for the design of sensor devices that maintain high sensitivity while optimizing manufacturing efficiency. This is crucial for improving the practicality of ZnO-based humidity sensors in commercial applications.

Keywords: ZnO Nanorods, Humidity Sensing, Growth Conditions, Hydrothermal Method, Sensor Optimization.

Introduction

Nanomaterials were first discovered with the introduction of carbon fullerenes in 1985 (Krätschmer et al., 1990), followed by the development of carbon nanotubes in 1991 (Ebbesen & Ajayan, 1992) and mesoporous materials in 1992 (Kresge et al., 1992). Nanomaterials have since played a critical role in sensor technology due to their unique

optical, electrical, and mechanical properties. These characteristics make them ideal for applications such as gas sensors, superconductors, photocatalysis, and optoelectronic devices (Chauhan, 2016; Kulkarni & Shirsat, 2015). Numerous studies have reported the use of nanomaterials as gas-sensitive elements, including zinc oxide (ZnO) (Spencer, 2012), titanium dioxide (TiO2) (Shimizu et al., 2002), tin oxide (SnO2) (Liu et al., 2015), indium oxide (In2O3) (Lai & Chen, 2012), and nickel oxide (NiO) (Lee et al., 2007). Among these materials, ZnO is particularly prominent in gas sensing due to its excellent chemical stability, electrical compatibility, high electron mobility, and biocompatibility (Anusha et al., 2014). As an n-type semiconductor, ZnO has a wide band gap of 3.37 eV and large exciton binding energy of 60 meV (Patil et al., 2016). Additionally, ZnO is easy to fabricate, cost-effective, and environmentally friendly, with strong optical transparency, particularly in the visible spectrum. This makes it highly suitable for short-wavelength optoelectronic devices (Ruchika & Kumar, 2015; Shinde et al., 2008; Tang et al., 2008), biosensors (Chang et al., 2010; Kong et al., 2009; Kumar & Chen, 2008), resonators (Cao et al., 1998), and medical devices (Rasmussen et al., 2010).

In optical sensing applications, ZnO is often used as a sensitive material to detect environmental parameters such as humidity, gas, or temperature. Its nanostructures provide a high surface-to-volume ratio, enhancing the adsorption of gas molecules on its surface (Suchorska-Woźniak et al., 2016). The adsorption and desorption of water molecules (humidity) change the electrical conductivity of ZnO, thereby modifying its optical properties (Rackauskas et al., 2017). This results in a measurable modulation of light transmission, corresponding to the environmental parameter being monitored. Relative humidity (RH), which refers to the concentration of water vapor in the air (Yeo et al., 2008), has significant implications for daily life, industrial processes, and health (Jiang et al., 2006). Accurate humidity monitoring is essential in fields such as food processing, agriculture, medical facilities, weather forecasting, and civil engineering (Khijwania et al., 2005; Shinzo et al., 2003; Zamarreño et al., 2010). While commercial electronic humidity sensors rely on changes in electrical conductivity or capacitance. They have limitations, such as electrical leakage due to water accumulation at high humidity levels. On the other hand, optical humidity sensors offer several advantages over conventional electronic sensors, including immunity to electromagnetic interference (Sabri et al., 2013) and the ability to transmit large amounts of sensor data over long distances with low attenuation (Lokman et al., 2016). These features make optical sensors ideal for critical applications, particularly in volatile or sensitive environments.

Several studies have optimized ZnO nanorod synthesis for humidity detection. However, most optimizations have focused on single parameters. For example, Hafiz et al. optimized humidity sensing based on ZnO nanorod growth duration, with 12 hours showing the highest sensitivity (Hafiz Jali et al., 2019). Batumalay et al. reported better humidity sensitivity in ZnO-seeded nanostructures on tapered optical fibers compared to non-seeded fibers (Batumalay et al., 2014). Rafis et al. optimized ZnO coating width for light-side coupling efficiency in alcohol vapor sensing, finding that the coating width of 5 mm produced the best results (Rahim et al., 2016). Despite these successes, sensing performance can be constrained by limitations in process parameters. The objective of this paper is to explore the flexibility of the ZnO fabrication process in achieving desired sensing performance independent of specific growth parameters. This study demonstrates the fabrication of ZnO nanorods on glass substrates

with variations in growth duration and coating length. The effect of ZnO growth conditions on optical scattering and humidity sensing performance is then analyzed.

Experimental Setup

ZnO Nanorods Synthesis via Hydrothermal Approach

In this experiment, standard microscopic glass substrates (Sail Brand model no. 7101) were cut into three pieces, each measuring 25 mm x 15 mm. The substrates were cleaned in a sequence of hydrochloric acid (HCl), sodium hydroxide (NaOH), soap water, ethanol, acetone, and deionized (DI) water. Each cleaning step was performed using an ultrasonic bath for 15 minutes to ensure the surfaces were completely free of stains, dirt, and dust. Afterward, the samples were dried in an atmospheric oven for 1 hour. To prepare for ZnO nanocrystallite deposition, the samples were masked with polytetrafluoroethylene (PTFE) tape, leaving a triangular area of 13 mm x 13 mm exposed. This triangular ZnO nanorod coating was specifically designed to evaluate the effect of coating length on light scattering and humidity sensing.

For the hydrothermal growth of ZnO nanorods, the exposed areas of the samples were first seeded with ZnO crystals (Baruah & Dutta, 2009a; Kitsomboonloha et al., 2009; Sugunan et al., 2006). A 1 mM seeding solution was prepared by dissolving zinc acetate (Zn(CH3COO)2) in ethanol (Fallah et al., 2013), and 50 µl of the solution was applied to the exposed triangular areas of the samples, which were heated to 70 °C. This process was repeated ten times which then followed by annealing procedure at 250 °C for 5 hours.

For nanorod growth, a precursor solution of 10 mM zinc nitrate hexahydrate (Zn(NO3)2·6H2O) and hexamethylenetetramine (HMT, (CH2)6N4) was prepared, following established hydrothermal methods (Baruah & Dutta, 2009a, 2009b; Promnimit et al., 2013). The seeded samples were placed face down in a Petri dish, leaving a gap between the sample and the dish surface, and submerged in the precursor solution. The samples were kept in a growth chamber at 90 °C for the durations of 5, 10, and 15 hours, based on optimal growth conditions from previous studies (Bora et al., 2014; Fallah et al., 2013; Hazli Rafis Bin Abdul et al., 2016; Rahim et al., 2016). The growth solution was discarded and replenished with a new solution for every 5 hours to maintain consistent nanorod growth (Baruah & Dutta, 2009b). After the growth process was completed, the samples were taken out and the masks were carefully removed. The ZnO-coated samples were then thoroughly rinsed with DI water and dried in an atmospheric oven. Post-annealing was conducted at 350 °C for 1 hour to remove any residual contaminants or defects from the ZnO nanorods (Bora et al., 2017). Finally, the microstructures of the ZnO nanorods on the glass substrate were examined using scanning electron microscopy (SEM, Hitachi SU5000 FE-SEM) at 20 kV.

Optical Characterization towards Humidity Sensing

Figure 1 illustrates the experimental setup used for the optical characterization and humidity measurement of the successfully fabricated samples. A controlled humidity chamber (0.35 m x 0.22 m x 0.23 m) was employed for all measurements. The coated samples were positioned on an automated translation stage controlled by a DC servo controller (Thorlabs APT-DC Servo Controller, model no.: TDC001), which was linked to a PC for control via a graphical user interface (GUI). A Thorlab LED light source with a central wavelength of 530 nm (Model no.: M530FI) was used, managed by a Thorlabs LED driver (Model no.: LEDD1B). The selection of

the green LED (530 nm) was based on previous studies conducted by our group, which indicated that this wavelength provided optimal sensing performance (Hazli Rafis Bin Abdul et al., 2016). The LED was positioned as close as possible to the edge of the coated glass substrate, while the photodetector was located at the opposite edge, allowing light to propagate from the LED to the photodiode within the glass substrate. The photodetector was connected to a Thorlabs power meter (Model no.: PM100USB), which was in turn linked to a PC for data recording. Additionally, a hygrometer was mounted on the chamber wall to continuously monitor the actual relative humidity (RH) level during the measurements.

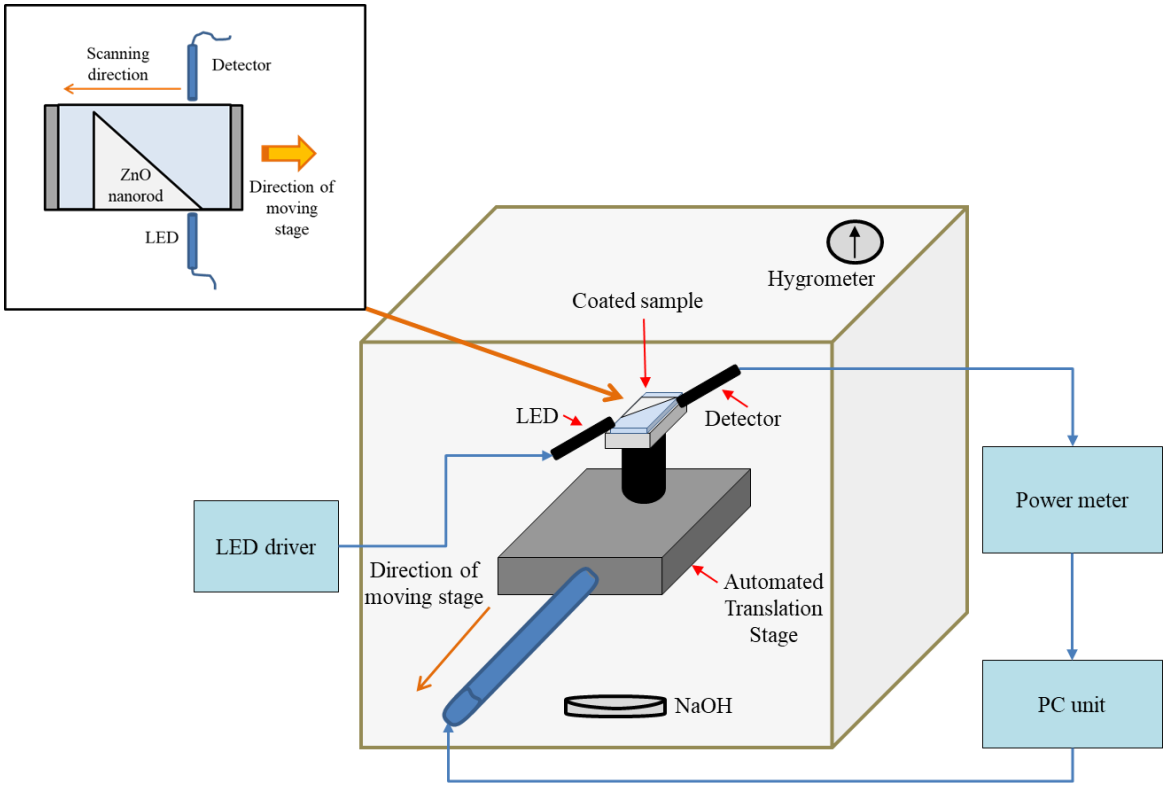

Figure 1: Schematic representation of the experimental setup for light scattering and humidity sensing measurement of the ZnO coated glass substrate. The inset shows the scanning direction for the light scattering measurement.

The first measurement focused on analyzing light scattering characteristics in relation to variations in coating lengths and growth durations. This analysis was conducted under ambient humidity conditions (50% RH) and a temperature of 25 °C. The automated translation stage was moved so that the coated glass substrate traveled horizontally between the LED and the photodetector, as depicted in the inset of Figure 1. During this process, light propagated from the LED through the glass substrate, allowing for the evaluation of different coating lengths. The output intensity power was recorded, and this measurement was repeated for all samples with varying growth durations.

Subsequently, the samples were characterized for humidity sensing. In this experiment, a mixture of NaOH and water was introduced into the humidity chamber to elevate the humidity level from the initial 50% (room level) to 80% RH, maintaining a constant temperature of 25 °C. As the chamber lid was closed, the humidity level was monitored, and

the output intensity power was recorded at each 5% increment in RH. Measurements were taken at four distinct points along the edge of the glass substrate, corresponding to four different ZnO coating lengths (1 mm, 4 mm, 7 mm, and 10 mm). This procedure was repeated for samples with varying growth times. The sensing response of each sample was analyzed by comparing the output intensity power recorded at each humidity level against the baseline measurement taken at 50% RH.

Result and Discussion

Characterization of the ZnO Nanorods Growth

Figure 2 presents optical images of the successfully coated glass substrates featuring triangular ZnO nanorods. Uniform ZnO coatings were observed across all glass substrates for growth processing times of 5 h, 10 h, and 15 h, as illustrated in Figures 2(a), 2(b), and 2(c), respectively. The sample with a 15 h growth duration exhibited the highest density of ZnO coatings compared to the 10 h and 5 h samples. Notably, the sample with 15 h growth time displayed the brightest white coating layer among all tested samples. In contrast, the sample with a 5 h growth duration demonstrated the lowest coating density, resulting in a more transparent layer than the other two samples. This suggests that varying growth processing times influence the characteristics of ZnO nanorods, including their diameter and length, which in turn affects the number of nanorods per unit area.

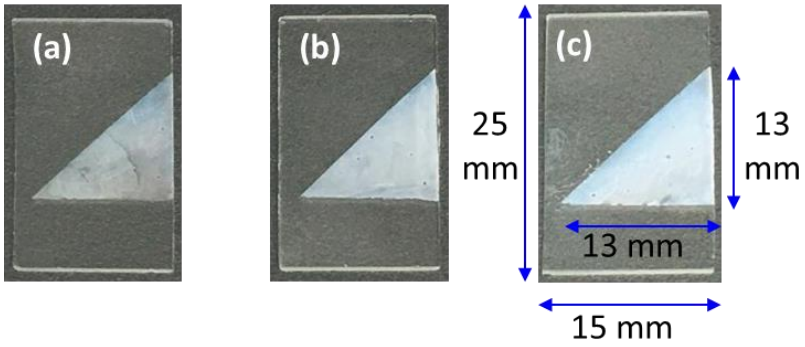

Figure 2: Uniform triangular shaped of ZnO nanorods coating on glass substrates for the growth processing times of (a) 5 h, (b) 10 h and (c) 15 h.

Figure 3 illustrates the microstructure of the ZnO nanorod coating layers on glass substrates as observed through scanning electron microscopy (SEM). All samples displayed hexagonal wurtzite ZnO nanorod structures, with Figures 3(a), 3(b), and 3(c) showcasing the top views for the samples with growth times of 5 h, 10 h, and 15 h, respectively. The diameter of the nanorods was found to increase significantly with longer growth durations, from 5 h to 15 h. The cross-sectional views of the ZnO coating layers are presented as insets in Figures 3(a), 3(b), and 3(c), revealing that the length of the nanorods also increased with longer growth times. Furthermore, it was noted that the nanorods in the sample with a 15 h growth duration exhibited better orientation compared to those in the 5 h and 10 h samples.

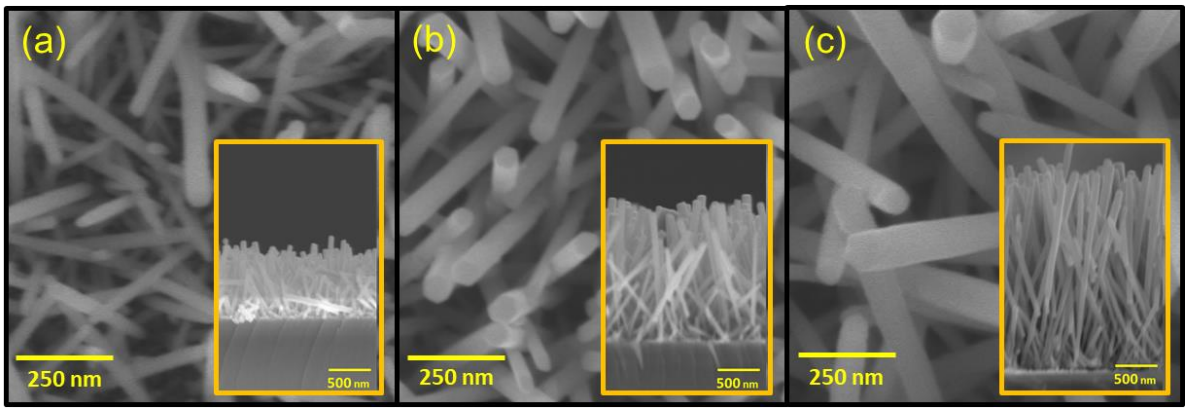

Figure 3: Top view of scanning electron micrographs of ZnO nanorods grown on glass substrate for growth times of (a) 5 h, 10 h and (c) 15 h. The inset in (a), (b) and (c) show the cross sectional of nanorods for the respective growth times.

Figure 4 provides comparative graphs illustrating the diameter, length, and number of nanorods per unit area across the different growth durations. The average diameter of the nanorods increased from 43 nm to 78 nm as the growth time extended from 5 h to 15 h, as shown in Figure 4(a). Correspondingly, the length of the nanorods also increased with growth time, measuring 0.85 µm, 1.62 µm, and 2.26 µm for the respective 5 h, 10 h, and 15 h growth periods. The average diameter and length of the nanorods were calculated by measuring multiple nanorods in each sample. However, a decreasing trend in the number of nanorods per unit area was observed, dropping from 1.4 x 10^{14} nanorods/m² to 5.7 x 10^{13} nanorods/m² as the growth time increased, as illustrated in Figure 4(c). This behavior can be attributed to the coalescence process during nanorod growth (Mohd Fudzi et al., 2018). As the nanorods became longer and larger, some of these nanorods merged to form larger nanorods structures, thereby reducing the number of individual nanorods per unit area.

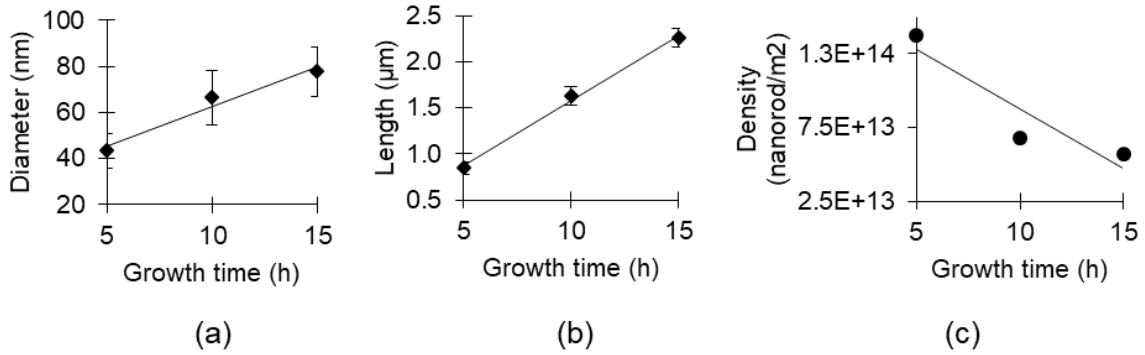

Figure 4: The comparison graph between the growth time for the (a) diameter, (b) length and (c) number of nanorods per unit area.

Optical Characterization of ZnO Nanorods Coated Glass Substrates

In the previous section, we examined how growth time influences the structural characteristics of nanorods, including their diameter, length, and the number of nanorods per unit area. Changes in these physical structures also lead to variations in the optical properties of the nanorods. Figure 5 displays the output intensity power measured by a power meter as it scans from 0 mm to 13 mm along the ZnO coating lengths for growth durations of 5 h, 10 h, and 15 h. This analysis allows for comparisons not only between different growth times but

also across varying coating lengths. The output power values were normalized against the optical power measured in the non-coated region (0 mm), which served as a reference point, as the output power values at 0 mm were nearly identical across all samples. The normalization was set to 1 W to maintain consistent units, as these values represent output power.

As illustrated in Figure 5, a decreasing trend in optical intensity was observed for all samples as the scan progressed from 0 mm to 13 mm along the coating lengths. ZnO is known to have a refractive index of approximately 2.00 (Bora et al., 2014), which is higher than the refractive index of a standard glass substrate (approximately 1.5). Before reaching the ZnO coating region, the guided light travelled at the glass-air interface at full intensity. However, upon encountering the glass-ZnO interface, some light was refracted due to the higher refractive index of ZnO, resulting in reduced intensity at the output. Consequently, a reduction in light intensity was first noted at the beginning of the ZnO coating (1 mm). With longer coating lengths, the guided light interacted with multiple glass-ZnO interfaces along its path, leading to further reductions in light intensity observed at 13 mm. Additionally, fluctuations in output power were recorded during the measurement from 0 mm to 13 mm, influenced by two main factors: the uniformity of the coating and the surface condition of the glass substrate where the light was excited. Although the ZnO coating appeared visually uniform, SEM images revealed variations in the physical size of the nanorods across the samples, affecting the leakage of light consistency. Furthermore, the glass cutting process was performed manually. The process did not guarantee a perfectly smooth edge which resulting in slight roughness that influenced light excitation within the glass. Nonetheless, the impact of the ZnO coating lengths remained evident, with output intensities decreasing as coating lengths increased, a trend consistent across all samples with varying growth durations. However, the extent of light leakage varied among samples due to differing nanorod microstructures based on growth processing times.

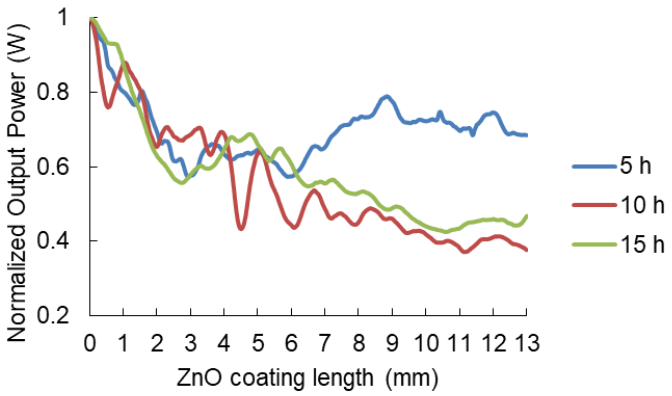

Figure 5: Optical characterization of the ZnO coated glass substrate on coating length variation for different growth durations.

The optical characterization comparison across growth times is also reflected in the graph presented in Figure 5. From the beginning to the end of the ZnO coating, it was observed that the sample with a 10 h growth time exhibited the highest rate of light leakage at -0.0437 W/mm. In contrast, the 5 h and 15 h samples demonstrated lower rates of light leakage at -0.0057 W/mm and -0.0323 W/mm, respectively. This suggests that the 10 h sample produced

a more pronounced scattering effect due to the ZnO nanorods. These results indicate that, aside from coating length, the amount of light leakage is also influenced by growth time. As previously discussed, the physical characteristics of the nanorod microstructures (diameter, length, and number of nanorods per unit area) are altered with varying growth times. In a first-order scattering model, where total scattering is considered a superposition of scattering from each rod, the intensity (*I*) over a distance *dx* of propagation is expressed as (Fallah et al., 2013)

$$\frac{dI}{dx} = -C_{sc}\rho_v I \tag{3.1}$$

where C_{sc} represents the scattering cross-section and ρ_v denotes the rod density per unit volume, $\rho_v = \rho_a/l$, and *l* being the average length of the nanorods. The scattering cross-section of a single rod is strongly dependent on its diameter, shape, and length. It is also important to note that intensity losses are influenced by both forward and backward scattering by the nanorods. In this study, forward scattering contributes to light leakage, while backward scattering reduces light losses by reflecting light back into the glass substrate. In cases where there is a higher density and longer nanorods, backward scattering predominates over forward scattering, enhancing output power towards the end of the glass substrate. Consequently, a slightly higher output power was observed at the end of the coating length for the 15 h sample compared to the 10 h sample.

The Effect of ZnO Nanorods Growth Conditions towards Humidity Sensing

Figure 6 illustrates the sensing response of glass substrates coated with ZnO nanorods against humidity detection. In this measurement, the optical transmittance difference (*ΔT*) indicates the amount of light received by the photodetector as humidity increases from 50% to 80% relative humidity (RH). The measured values were normalized against the reference value of the initial RH (50%). Overall, the results demonstrate that the sensing response becomes increasingly negative with longer ZnO nanorods coating lengths across all samples grown for 5 h, 10 h, and 15 h. While the general trend indicates that coating length influences the sensing response, the sample with a 5 h growth time showed unstable responses, particularly at the 1 mm, 4 mm, and 7 mm regions, as depicted in Figure 6(a). This instability is attributed to the inadequately developed nanorod structures for the 5 h growth duration, which were shorter and less uniform, as evidenced by the SEM image in Figure 3(a). Consequently, inconsistent readings were recorded for this sample. However, a significant trend in humidity sensing was observed at the 10 mm coating length. In contrast, the samples grown for 10 h and 15 h as shown in Figures 6(b) and 6(c), respectively exhibited improved consistency in sensing responses due to the enhanced elongation of the ZnO nanorods compared to the 5 h sample. Both of these samples demonstrated substantial sensing responses across different coating lengths, with the highest sensing responses consistently occurring at 10 mm of coating length when tested at maximum humidity. This finding suggests that a larger ZnO coating area provides an increased sensing surface, significantly enhancing both the sensing response and sensitivity.

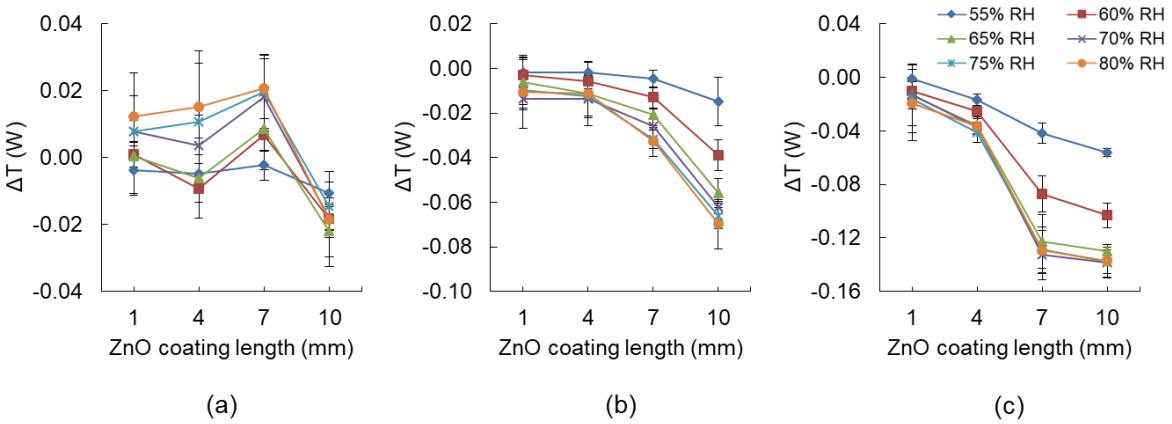

Figure 6: Humidity sensing response on ZnO coated glass substrates for the growth durations of (a) 5 h, (b) 10 h and (c) 15 h.

In addition to the influence of ZnO coating length, growth duration is a critical factor in humidity sensing performance. Figure 6 indicates that the sensing response for the sample with a 15 h growth time was significantly greater across all coating lengths. As shown in the SEM images in Figure 3, the nanorods in the 15 h sample have the largest diameter and length. The physical dimensions of the nanorods play a vital role in sensing performance. The sensing mechanism of the ZnO nanorods is based on the adsorption and desorption of water molecules on their surfaces (Kim et al., 2005). When exposed to humid air, water molecules adhere to the nanorods' surfaces. The oxygen adsorbed on the rods becomes negatively charged, extracting electrons from the ZnO surface (Rackauskas et al., 2017). This interaction creates a depletion layer of surface charge due to electron losses, affecting the effective conduction channel of the ZnO material. As a result, the electrical conductivity of the material changes, which in turn alters its complex refractive index. Changes in the refractive index affect the optical characteristics of the ZnO and modify the scattering patterns of the nanorods. This experiment demonstrates that a longer growth duration (15 h) combined with a larger coating section (10 mm) yields the highest sensing response overall.

While these conditions may yield the highest sensing response, they do not necessarily represent the optimal settings. It is essential to recognize that two parameters are involved in this characterization, both of which can be adjusted to achieve similar sensing performance. Figure 7 summarizes the sensing responses measured at 80% RH for all samples (grown with 5 h, 10 h, and 15 h) across various coating lengths (1 mm, 4 mm, 7 mm, and 10 mm). Notably, similar sensing responses can be achieved with different combinations of parameter settings as highlighted in red circle in Figure 7. For example, a sensing response of -0.0326 W was recorded for the combination of 10 h growth time and 7 mm coating length, while the combination of 15 h growth time and 4 mm coating length yielded -0.0366 W, as summarized in the inset of Figure 7.

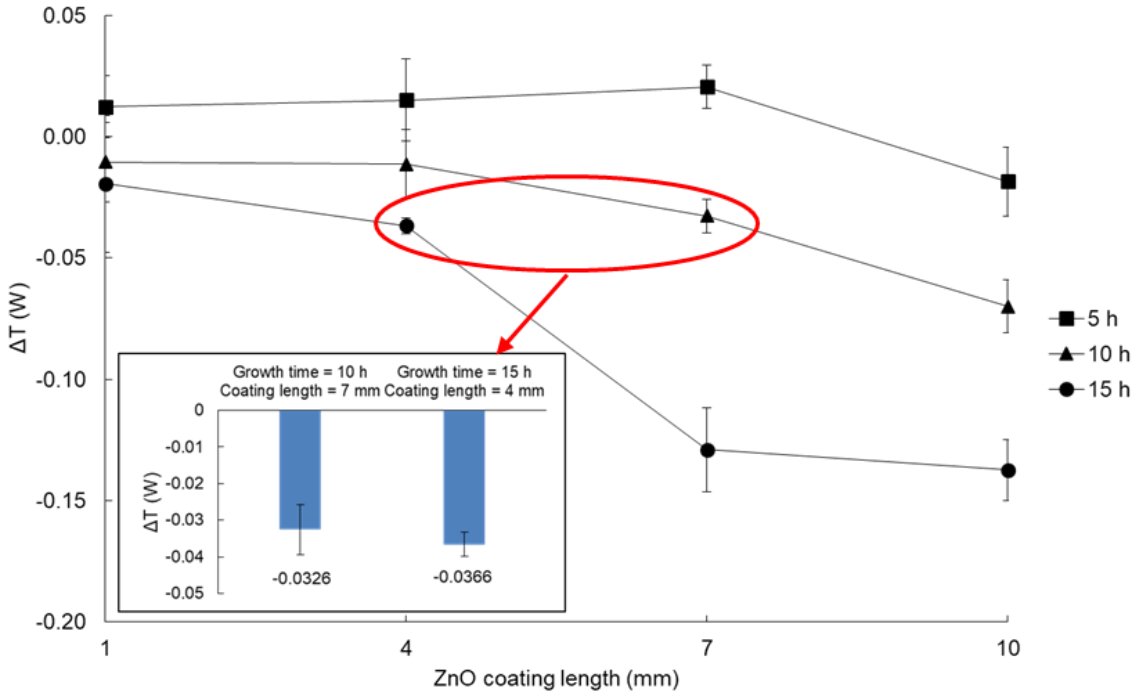

Figure 7: Summary of humidity response on glass substrates on ZnO coating variations (growth time and coating length). The inset shows the comparison between two different growth settings producing almost identical sensing response.

This experiment demonstrates that although the 10 h sample, which underwent a shorter growth time, it still can achieve high sensing performance due to its longer coating length providing increased light interaction with the glass-ZnO interfaces. The optimum sensing performance is not solely dependent on a single parameter, such as ZnO nanorods growth time or coating length. According to the Beer-Lambert principle, the intensity of light received by the photodetector is given by (Husain et al., 2013)

$$I = I_0 e^{-\alpha x} \tag{3.2}$$

where I_0 and I are the light intensities entering and exiting the medium, respectively, α is the absorption coefficient of the medium, and x is the thickness of the medium through which light propagates. This principle can be applied to this investigation by substituting α with the scattering coefficient of the ZnO nanorods and x with the length of the coating region. The scattering caused by humidity effects is heavily influenced by these two parameters. Each parameter exhibits its own scattering rate based on characteristics like growth duration or coating length. Therefore, these parameters can be dynamically adjusted to achieve the desired sensing response according to fabrication process requirements.

Conclusion

This study explored the influence of growth duration and coating length on the humidity sensing capabilities of glass substrates coated with ZnO nanorods. The findings revealed that varying growth configurations can yield nearly equivalent sensing performance. Specifically, the combination of a 10-hour growth time with a 7 mm coating length demonstrated a sensing response similar to that of a 15-hour growth time with a 4 mm coating length, yielding approximately -0.0326 W and -0.0366 W, respectively, at 80% relative humidity. While the

optimal sensing response was observed with a 15-hour growth duration and a 10 mm coating length, this research highlights the potential for achieving comparable sensing results by adjusting these two parameters. Consequently, this suggests that strict optimization based solely on specific fabrication parameters may not be the most effective approach for sensor design. Instead, adopting a more flexible fabrication process could provide significant advantages in sensor development, particularly in terms of time and cost efficiency.

Acknowledgements

The authors wish to express their gratitude to the Faculty of Electronics and Computer Technology and Engineering (FTKEK), the Center for Research and Innovation Management (CRIM), Universiti Teknikal Malaysia Melaka (UTeM), and the Faculty of Engineering, University of Malaya, for their support in providing financial and laboratory facilities for this research.

References

Anusha, J. R., Kim, H.-J., Fleming, A. T., Das, S. J., Yu, K.-H., Kim, B. C., & Raj, C. J. (2014). Simple fabrication of ZnO/Pt/chitosan electrode for enzymatic glucose biosensor. *Sensors and Actuators B: Chemical*, *202*, 827-833. https://doi.org/https://doi.org/10.1016/j.snb.2014.06.024

Baruah, S., & Dutta, J. (2009a). Effect of seeded substrates on hydrothermally grown ZnO nanorods. *Journal of Sol-Gel Science and Technology*, *50*(3), 456-464. https://doi.org/10.1007/s10971-009-1917-2

Baruah, S., & Dutta, J. (2009b). Hydrothermal growth of ZnO nanostructures. *Science and Technology of Advanced Materials*, *10*(1), 013001. https://doi.org/10.1088/1468-6996/10/1/013001

Batumalay, M., Harith, Z., Rafaie, H. A., Ahmad, F., Khasanah, M., Harun, S. W., Nor, R. M., & Ahmad, H. (2014). Tapered plastic optical fiber coated with ZnO nanostructures for the measurement of uric acid concentrations and changes in relative humidity. *Sensors and Actuators A: Physical*, *210*, 190-196. https://doi.org/https://doi.org/10.1016/j.sna.2014.01.035

Bora, T., Fallah, H., Chaudhari, M., Apiwattanadej, T., Harun, S. W., Mohammed, W. S., & Dutta, J. (2014). Controlled side coupling of light to cladding mode of ZnO nanorod coated optical fibers and its implications for chemical vapor sensing. *Sensors and Actuators B: Chemical*, *202*, 543-550. https://doi.org/https://doi.org/10.1016/j.snb.2014.05.097

Bora, T., Sathe, P., Laxman, K., Dobretsov, S., & Dutta, J. (2017). Defect engineered visible light active ZnO nanorods for photocatalytic treatment of water. *Catalysis Today*, *284*, 11-18. https://doi.org/https://doi.org/10.1016/j.cattod.2016.09.014

Cao, H., Zhao, Y. G., Ong, H. C., Ho, S. T., Dai, J. Y., Wu, J. Y., & Chang, R. P. H. (1998). Ultraviolet lasing in resonators formed by scattering in semiconductor polycrystalline films. *Applied Physics Letters*, *73*(25), 3656-3658. https://doi.org/10.1063/1.122853

Chang, C.-C., Chiu, N.-F., Lin, D. S., Chu-Su, Y., Liang, Y.-H., & Lin, C.-W. (2010). High-Sensitivity Detection of Carbohydrate Antigen 15-3 Using a Gold/Zinc Oxide Thin Film Surface Plasmon Resonance-Based Biosensor. *Analytical Chemistry*, *82*(4), 1207-1212. https://doi.org/10.1021/ac901797j

Chauhan, P. (2016). Nanomaterials for Sensing Applications. *Journal of Nanomedicine Research*, *3*(5). https://doi.org/10.15406/jnmr.2016.03.00067

Ebbesen, T. W., & Ajayan, P. M. (1992). Large-scale synthesis of carbon nanotubes. *Nature*, *358*(6383), 220-222. https://doi.org/10.1038/358220a0

Fallah, H., Chaudhari, M., Bora, T., Harun, S. W., Mohammed, W. S., & Dutta, J. (2013). Demonstration of side coupling to cladding modes through zinc oxide nanorods grown on multimode optical fiber. *Optics Letters*, *38*(18), 3620-3622. https://doi.org/10.1364/OL.38.003620

Hafiz Jali, M., Rafis Abdul Rahim, H., Helmi Mohd Yusof, H., Md Johari, M. A., Thokchom, S., & Wadi Harun, S. (2019). Optimization of ZnO nanorods growth duration for humidity sensing application. *Journal of Physics: Conference Series*, *1371*(1), 012005. https://doi.org/10.1088/1742-6596/1371/1/012005

Hakimi, H., & Nabilah, A. (2024). Book Recommendation System (BRS) Using Collaboration Filtering Machine Learning. In *Opportunities and Risks in AI for Business Development: Volume 1* (pp. 993-1002). Cham: Springer Nature Switzerland.

Hazli Rafis Bin Abdul, R., Muhammad Quisar Bin, L., Sulaiman Wadi, H., Gabor Louis, H., Karel, S., Waleed Soliman, M., & Joydeep, D. (2016). Applied light-side coupling with optimized spiral-patterned zinc oxide nanorod coatings for multiple optical channel alcohol vapor sensing. *Journal of Nanophotonics*, *10*(3), 036009. https://doi.org/10.1117/1.JNP.10.036009

Husain, I., Choudhury, A., & Nath, P. (2013). Fiber-Optic Volumetric Sensor Based on Beer-Lambert Principle. *IEEE Sensors Journal*, *13*(9), 3345-3346. https://doi.org/10.1109/JSEN.2013.2272795

Ismail, N. F., Akmal, S., Mohd, Massila Kamalrudin, Amirul Affiq, Hakimi, H., & Azmi, S. S. (2024). Agile Decision-Making as an Alternative for Decision Making's Complexities in Information Management to Flood Rescue and Recovery: A Systematic Literature Review. Journal of Advanced Research in Applied Sciences and Engineering Technology, 89–105. https://doi.org/10.37934/araset.58.1.89105

Jiang, T., Zhou, X., Zhang, J., Zhu, J., Li, X., & Li, T. (2006, 22-25 Oct. 2006). Study of humidity properties of Zinc Oxide modified Porous Silicon. SENSORS, 2006 IEEE,

Khijwania, S., Srinivasan, K., & Singh, J. (2005). Performance optimized optical fiber sensor for humidity measurement. *Optical Engineering - OPT ENG*, *44*. https://doi.org/10.1117/1.1870753

Kim, H. K., Sathaye, S., Hwang, Y. K., Jhung, S. H., Hwang, J. S., Kwon, S. H., Park, S.-E., & Chang, J. (2005). Humidity Sensing Properties of Nanoporous TiO2-SnO2 Ceramic Sensors. *Bulletin- Korean Chemical Society*, *26*, 1881-1884. https://doi.org/10.5012/bkcs.2005.26.11.1881

Kitsomboonloha, R., Baruah, S., Myint, M. T. Z., Subramanian, V., & Dutta, J. (2009). Selective growth of zinc oxide nanorods on inkjet printed seed patterns. *Journal of Crystal Growth*, *311*(8), 2352-2358. https://doi.org/https://doi.org/10.1016/j.jcrysgro.2009.02.028

Kong, T., Chen, Y., Ye, Y., Zhang, K., Wang, Z., & Wang, X. (2009). An amperometric glucose biosensor based on the immobilization of glucose oxidase on the ZnO nanotubes. *Sensors and Actuators B: Chemical*, *138*(1), 344-350. https://doi.org/https://doi.org/10.1016/j.snb.2009.01.002

Krätschmer, W., Lamb, L. D., Fostiropoulos, K., & Huffman, D. R. (1990). Solid C60: a new form of carbon. *Nature*, *347*(6291), 354-358. https://doi.org/10.1038/347354a0

Kresge, C. T., Leonowicz, M. E., Roth, W. J., Vartuli, J. C., & Beck, J. S. (1992). Ordered mesoporous molecular sieves synthesized by a liquid-crystal template mechanism. *Nature*, *359*(6397), 710-712. https://doi.org/10.1038/359710a0

Kulkarni, S. S., & Shirsat, M. D. (2015). Optical and structural properties of zinc oxide nanoparticles. *International Journal of Advanced Research in Physical Science*, *2*(1), 14-18.

Kumar, S. A., & Chen, S. M. (2008). Nanostructured Zinc Oxide Particles in Chemically Modified Electrodes for Biosensor Applications. *Analytical Letters*, *41*(2), 141-158. https://doi.org/10.1080/00032710701792612

Lai, H.-Y., & Chen, C.-H. (2012). Highly sensitive room-temperature CO gas sensors: Pt and Pd nanoparticle-decorated In2O3 flower-like nanobundles [10.1039/C2JM31180A]. *Journal of Materials Chemistry*, *22*(26), 13204-13208. https://doi.org/10.1039/C2JM31180A

Lee, C.-Y., Chiang, C.-M., Wang, Y.-H., & Ma, R.-H. (2007). A self-heating gas sensor with integrated NiO thin-film for formaldehyde detection. *Sensors and Actuators B: Chemical*, *122*(2), 503-510. https://doi.org/https://doi.org/10.1016/j.snb.2006.06.018

Liu, C., Kuang, Q., Xie, Z., & Zheng, L. (2015). The effect of noble metal (Au, Pd and Pt) nanoparticles on the gas sensing performance of SnO2-based sensors: a case study on the {221} high-index faceted SnO2 octahedra [10.1039/C5CE01162K]. *CrystEngComm*, *17*(33), 6308-6313. https://doi.org/10.1039/C5CE01162K

Lokman, A., Arof, H., Harun, S. W., Harith, Z., Rafaie, H. A., & Nor, R. M. (2016). Optical Fiber Relative Humidity Sensor Based on Inline Mach–Zehnder Interferometer With ZnO Nanowires Coating. *IEEE Sensors Journal*, *16*(2), 312-316. https://doi.org/10.1109/JSEN.2015.2431716

Mohd Fudzi, L., Zainal, Z., Lim, H. N., Chang, S.-K., Holi, A. M., & Sarif@Mohd Ali, M. (2018). Effect of Temperature and Growth Time on Vertically Aligned ZnO Nanorods by Simplified Hydrothermal Technique for Photoelectrochemical Cells. *Materials*, *11*(5).

Patil, Y. S., Raghuvanshi, F., & Patil, I. (2016). Zinc oxide nanorods as H 2 S gas sensor. *Int. J. Sci. Res.*, *5*(7), 1140-1144.

Promnimit, S., Baruah, S., Lamdu, U., & Dutta, J. (2013). Hydrothermal Growth of ZnO Hexagonal Nanocrystals: Effect of Growth Conditions. *Journal of Nano Research*, *21*, 57-63. https://doi.org/10.4028/www.scientific.net/JNanoR.21.57

Rackauskas, S., Barbero, N., Barolo, C., & Viscardi, G. (2017). ZnO Nanowire Application in Chemoresistive Sensing: A Review. *Nanomaterials*, *7*(11).

Rahim, H. R. B. A., Manjunath, S., Fallah, H., Thokchom, S., Harun, S. W., Mohammed, W. S., Hornyak, L. G., & Dutta, J. (2016). Side coupling of multiple optical channels by spiral patterned zinc oxide coatings on large core plastic optical fibers. *Micro & Nano Letters*, *11*(2), 122-126. https://doi.org/https://doi.org/10.1049/mnl.2015.0452

Rasmussen, J. W., Martinez, E., Louka, P., & Wingett, D. G. (2010). Zinc oxide nanoparticles for selective destruction of tumor cells and potential for drug delivery applications. *Expert Opin Drug Deliv*, *7*(9), 1063-1077. https://doi.org/10.1517/17425247.2010.502560

Ruchika, & Kumar, A. (2015). Performance analysis of Zinc oxide based alcohol sensors. *International Journal of Applied Science and Engineering Research*, *4*, 427-436.

Sabri, N., Aljunid, S. A., Salim, M. S., Ahmad, R. B., & Kamaruddin, R. (2013). Toward Optical Sensors: Review and Applications. *Journal of Physics: Conference Series*, *423*(1), 012064. https://doi.org/10.1088/1742-6596/423/1/012064

Shimizu, Y., Kuwano, N., Hyodo, T., & Egashira, M. (2002). High H2 sensing performance of anodically oxidized TiO2 film contacted with Pd. *Sensors and Actuators B: Chemical*, *83*(1), 195-201. https://doi.org/https://doi.org/10.1016/S0925-4005(01)01040-1

Shinde, S. S., Shinde, P. S., Bhosale, C. H., & Rajpure, K. Y. (2008). Optoelectronic properties of sprayed transparent and conducting indium doped zinc oxide thin films. *Journal of Physics D: Applied Physics*, *41*(10), 105109. https://doi.org/10.1088/0022-3727/41/10/105109

Shinzo, M., Osamu, S., Takashi, A., & Masayuki, M. (2003). A plastic optical fibre sensor for real-time humidity monitoring. *Measurement Science and Technology*, *14*(6), 746. https://doi.org/10.1088/0957-0233/14/6/306

Spencer, M. J. S. (2012). Gas sensing applications of 1D-nanostructured zinc oxide: Insights from density functional theory calculations. *Progress in Materials Science*, *57*(3), 437-486. https://doi.org/https://doi.org/10.1016/j.pmatsci.2011.06.001

Suchorska-Woźniak, P., Nawrot, W., Rac, O., Fiedot, M., & Teterycz, H. (2016). Improving the sensitivity of the ZnO gas sensor to dimethyl sulfide. *IOP Conference Series: Materials Science and Engineering*, *104*(1), 012030. https://doi.org/10.1088/1757-899X/104/1/012030

Sugunan, A., Warad, H. C., Boman, M., & Dutta, J. (2006). Zinc oxide nanowires in chemical bath on seeded substrates: Role of hexamine. *Journal of Sol-Gel Science and Technology*, *39*(1), 49-56. https://doi.org/10.1007/s10971-006-6969-y

Tang, C.-F., Kumar, S. A., & Chen, S.-M. (2008). Zinc oxide/redox mediator composite films-based sensor for electrochemical detection of important biomolecules. *Analytical Biochemistry*, *380*(2), 174-183. https://doi.org/https://doi.org/10.1016/j.ab.2008.06.004

Yeo, T. L., Sun, T., & Grattan, K. T. V. (2008). Fibre-optic sensor technologies for humidity and moisture measurement. *Sensors and Actuators A: Physical*, *144*(2), 280-295. https://doi.org/https://doi.org/10.1016/j.sna.2008.01.017

Yusof, Junaidah & d'Arqom, Annette & Surjaningrum, Endang & Panatik, Siti & Noor, Sabariah & Jalil, Nurul Iman & Harun, Mohd & Hakimi, Halimaton. (2025). The psychosocial factors of blood donation during the pandemic: Strategies for sustainable blood supply. Journal of Infrastructure, Policy and Development. 9. 9677. 10.24294/jipd9677.

Zamarreño, C. R., Hernaez, M., Del Villar, I., Matias, I. R., & Arregui, F. J. (2010). Tunable humidity sensor based on ITO-coated optical fiber. *Sensors and Actuators B: Chemical*, *146*(1), 414-417. https://doi.org/https://doi.org/10.1016/j.snb.2010.02.029